CHEMICAL ENGINEERING TRANSACTIONS
VOL. 100, 2023
A publication of AIDIC
The Italian Association of Chemical Engineering
Online at www.cetjournal.it
Guest Editors: Sauro Pierucci, Flavio Manenti

ISBN 979-12-81206-03-8; **ISSN** 2283-9216
DOI: 10.3303/CET23100055

CFD Analysis of Inline Mixing of Non-Ideal Liquid Mixtures

Riccardo Bacci di Capaci*, Marzia Doneddu, Elisabetta Brunazzi, Gabriele Pannocchia, Chiara Galletti

Department of Civil and Industrial Engineering, University of Pisa, Largo Lucio Lazzarino 2, 56122, Pisa, Italy
riccardo.bacci@ing.unipi.it

Numerical simulations based on Computational Fluid Dynamics have been performed for the assisted design of the flexible and transportable flow reactor developed within the Turboflux project. The core of the system consists of a tubular pipe, carrying the main fluids, and multiple injection ducts for the additive components. Mixing is ensured by a series of static mixing elements fitted within the main pipe. More specifically, we focus herein on the production of the sanitizing gel, obtained from three main components, i.e., ethanol, water, and glycerol. Hence, the numerical code is customized by implementing the non-ideal behaviour of the mixture. The degree of mixing and pressure drops are estimated in a wide range of scenarios, covering different flow regimes. The analysis allows one to identify the optimal operating conditions and, also, to put the basis for the setup of a digital twin of the system.

1. Introduction

As one of the most important operations in the process industry, the mixing process has been widely investigated in the literature. In general, stirred tanks are the most used equipment, which allows an efficient blending of liquids (Paul et al., 2004). Nevertheless, for several applications, various issues emerge related to the energy consumption of moving elements, the need for large volumes and control specifications, which results in large units and high operating costs (Myers et al., 1997). One of the objectives of process intensification is to find more efficient, less energy-intensive systems which imply lower space and require simpler control systems, which ultimately lead to a lower overall cost, both in economic and environmental terms (Sengupta and Yelvington, 2020).

Static mixers, introduced in ‘70s, are now standard equipment in the process industry as an alternative to mechanical agitators. These mixing devices, consisting of a series of repeated fixed inserts, are installed directly inside pipes and allow fluids to distribute transversely to the main flow direction, thus promoting concentration homogeneity with a very increase of mass and heat transfer and hence the process efficiency (Thakur et al., 2003). They give considerable economic advantages, as lower energy consumption, volumes reduction, and process transformation from batch to continuous mode. To date, many industrial patents and scientific papers describe the performance of various types of static mixers with reference to the type of fluids to be mixed. The possibility to easily change the layout of the internal elements allows one to optimize the configuration for the specific applications and flow regimes (Ghanem et al., 2014; Forte et al., 2019).

The fluid redistribution efficiency is strictly dependent on the specific design and the number of elements installed; manufacturers provide a lot of experimental data with common liquids describing performance for different applications, so the use of standard design is recommended. However, when mixing non-ideal liquids, we have to carry out additional experimental tests to evaluate the mixing efficiency and determine the most suitable type of static mixers. To this aim, Computational Fluid Dynamics (CFD) analysis is a powerful tool for the preliminary evaluation of static mixer performance, able to replace direct experimentation to reduce times and new design costs. By CFD it is also possible to obtain data with a high level of resolution to quantify the main reference design parameters (Antognoli et. al., 2019).

The present study thus aims at characterizing the performance of static mixers of Ross LPD type installed on an in-line reactor to produce different chemical formulates. In particular, the degree of mixing and pressure drops related to the mixing of basic components of the sanitizing gel, i.e., ethanol, water, and glycerol, are

Paper Received: 11 December 2022; Revised: 24 April 2023; Accepted: 29 May 2023
Please cite this article as: Bacci Di Capaci R., Marzia D., Brunazzi E., Pannocchia G., Galletti C., 2023, CFD Analysis of Inline Mixing of Non-ideal Liquid Mixtures, Chemical Engineering Transactions, 100, 325-330 DOI:10.3303/CET23100055

evaluated through numerical simulations. Ethanol is referred as the “carrier fluid" and water or glycerol as the "additive fluid". The standard CFD code of ANSYS Fluent v20 is upgraded by implementing the non-ideal behaviour of the mixture. The remainder of the paper is as follows: Section 2 briefly presents the case study; in Section 3 models and methods are illustrated, while in Section 4 results and relative discussion are given. Finally, conclusions are drawn in Section 5.

2. The case study

To properly analyse the mixing behaviour of the non-ideal liquid mixture, main geometrical characteristics of the real in-line reactor are firstly considered. The main pipe has an internal diameter D = 80 mm and a length of around 20 m where 8 series of Ross LPD static mixers are installed. The various static mixers consist of a repetitive unit of 5 elements, alternately rotated by 45 ° with respect to the axis of the central support shaft; each element has two complementary and orthogonal semi-elliptical plates, sized 106 x 38.5 mm. This mechanical solution is useful for both laminar and turbulent regimes and has no viscosity limits. The additive fluids are progressively injected from pipes with an internal diameter of 25 mm, inclined by 45 ° with respect to the main pipe. In this paper, only the two repetitive units of the real plant are considered. The simplified geometric models, developed under thin-wall hypothesis, are shown in Figure 1. The additive fluid injection section is 0.9 m length for the main pipe and 0.17 m for the additive fluid; the mixing section with static mixers is of 1 m length.

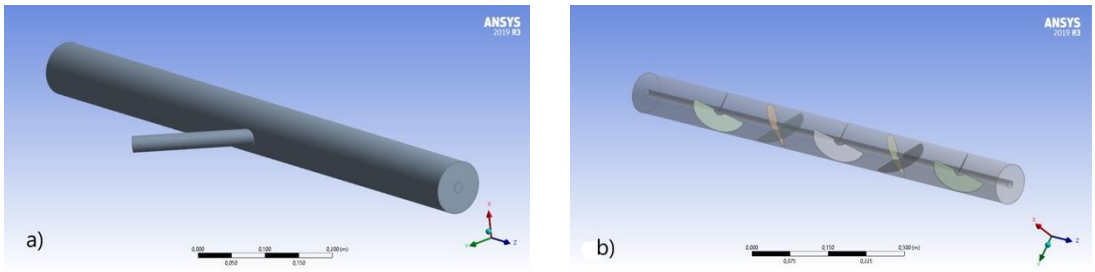

Figure 1: The geometrical models under study: a) additive fluid injection section; b) mixing section

This work focused on the mixing characteristics of the three basic components of the sanitizing gel, i.e., ethanol, water, and glycerol. Mixing is assumed between pure components to simulate the worst-case conditions. In particular, the behaviour of two binary mixtures is here discussed: i) ethanol-water (E-W), and ii) ethanol-glycerol (E-G). In addition, the ethanol-ethanol (E-E) mixture was also analysed as reference mixture. The volumetric flow rate of the carrier fluid is fixed and equal to 200 L/min; three levels of flow rate for the additive fluid, i.e., water or glycerol, are considered: 1-10-20 L/min. Note that non-ideal mixing scenarios are investigated, that is, mixture real properties are considered. In details, density and viscosity for E-W and E-G mixtures were implemented as User-Defined Functions (UDFs). More specifically, we adopted polynomial functions in terms of mass fraction of the two components, obtained from the interpolation of experimental data, i.e., from Orsi et al. (2013) for the E-W mixture, from Alkindi et al. (2008) for the E-G mixture.

3. Models and Methods

The numerical models used in this work are based on the following assumptions: single-phase systems, mixing of incompressible fluids, isothermal conditions, and absence of chemical reactions. The fluids flow field can be then described by Navier-Stokes equations:

$$\frac{\partial \rho}{\partial t} + \nabla(\rho u) = 0 \tag{1}$$

$$\frac{D\rho u}{Dt} = \frac{\partial \rho u}{\partial t} + \nabla(\rho u u) = -\nabla P - \nabla(\mu \nabla u) + \rho g \tag{2}$$

where u is the velocity vector, P the pressure, ρ the density, μ the viscosity and ∇ the gradient operator. A transport equation for the additive fluid is also considered, i.e.:

$$\frac{\partial \rho y_t}{\partial t} + \nabla(\rho u y_t) = \nabla(\rho D_t \nabla y_t) \tag{3}$$

where y_t is the additive mass fraction and D_t is the additive molecular diffusivity with respect to the carrier fluid. The various systems are modelled and solved numerically using the Reynolds-Averaged Navier-Stokes (RANS) equations and, since the mixing occurs under turbulent conditions, the closure of the unknown terms is performed with the k-ω SST model which best describes vortex motions (Kuntz et. al, 2003). This model

introduces turbulent variables as boundary conditions; in particular, the hydraulic diameter D_{eq}, here assumed as the pipe internal diameter D, and the turbulence intensity TI, defined as $TI = \sqrt{(2k/3)}/U$, where k is the turbulent kinetic energy and U is the mean velocity, and calculated with the empirical correlation valid for fully developed flows in pipes as $TI = 0.16Re^{-(1/8)}$.

To properly consider the additive fluid mass fraction and, therefore, include its transport equation, a suitable User-Defined Scalar (UDS) was used, which is also necessary for the definition of non-ideal mixture properties (i.e., viscosity and density). Furthermore, since the mixing is carried out under turbulent regime conditions, turbulent diffusivity is introduced, and described by the gradient transport hypothesis, with a suitable UDF, as: $D_t = \rho D + (\mu_t/Sc_t)$, where μ_t is the turbulent viscosity and Sc_t is the turbulent Schmidt number, assumed empirically equal to 0.7 (Montante et al., 2016).

For the problem resolution, suitable boundary conditions (BC) must be imposed. The carrier fluid flows in turbulent regime, therefore, its velocity profile has been initialized with a suitable turbulent profile, developed in a preliminary simulation where pure ethanol flows in an empty pipe 10D long. For the inlet of fluids, *velocity inlet* BC is used with a turbulent profile for the main pipe and a uniform velocity magnitude for the injection pipe, and a specified value for UDS, TI and D_{eq}; whereas the *Outflow* BC is imposed at the outlet of an additional empty pipe 1 m long just used to avoid backflow conditions and corrupted results in velocity and pressure fields.

Before main CFD simulations, a study of the independence of the results from the computational grid was carried out. For simplicity, the analysis evaluated six grids with different maximum dimension of the tetrahedral cell under laminar flow regime. The comparison was performed taking as parameters the velocity module on an axial chord, the velocity module on a radial chord, and the absolute pressure on different cross-sections. The study was conducted on both the additive fluid injection section and the mixing section. The optimal maximum size cell was thus selected as 2 mm, for both sections. For the main CFD simulations, a maximum-size mesh of 2 mm was then used, but with polyhedral cells and a 3-prism layer at the walls.

The CFD results were then post-processed to obtain suitable design parameters. In particular, the degree of mixing and the pressure drops were considered. The degree of mixing indicates the mixing efficiency, and in the case of a binary mixture is defined as (Orsi et al., 2013):

$$\sigma_b^2(z) = \frac{1}{N\underline{\rho}\underline{u}}\sum_{i=1}^{N}(\phi_i - \underline{\phi}_b)^2\rho_i u_i \tag{4}$$

$$\sigma_{max} = \sqrt{\underline{\phi}_b(1-\underline{\phi}_b)} \tag{5}$$

$$\delta_{mix}(z) = 1 - \frac{\sigma_b}{\sigma_{max}} \tag{6}$$

where σ_b^2 is the variance of the local mass fraction ϕ; $\underline{\phi}_b$ is the mean mass fraction of the reference fluid in the bulk; ϕ_i, ρ_i and u_i are the mass fraction, density, and axial velocity of fluid in the i-th cell, respectively; σ_{max} is the maximum value of the standard deviation σ_b; N is the number of measurements (i.e., cells), within the considered pipe cross-section; $\underline{\rho}$ and $\underline{u}$ are averaged density and velocity of the bulk. Note that the degree of mixing varies along the axial coordinate z, the main flow direction.

Static mixers typically increase the pressure drop per unit length of pipeline with respect to the empty pipe from 5 to 100 times, depending on the mixer geometry and flow conditions. To this aim, the absolute pressure was monitored, as the surface integral of the pressure (i.e., area weighted average, AWA), at different cross-sections:

$$AWA_P(z) = \frac{1}{A}\sum_{i=1}^{N} P_i|A_i| \tag{7}$$

where P_i and A_i are, respectively, the local pressure and the area, at a fixed coordinate z, of the i-th cell. The difference between the mean inlet and outlet pressure determines the total head loss.

4. Results and Discussion

The results obtained from the CFD simulations were analysed qualitatively and quantitatively. As first step, velocity and concentration fields were investigated. Data obtained on suitable cross-sections have been considered. In Figure 2 the velocity fields for the E-W and E-G mixtures for the case of 10 L/min of additive flow rate are reported. For both mixtures, a significant variation in the velocity profile is observed, from the initial injection section of the additive to the core mixing section; the velocity modulus increases close to the pipe walls and then propagates inwards. For both mixtures, the velocity modulus increases as the additive flow rate increases, but this effect is not here illustrated in detail for the sake of brevity.

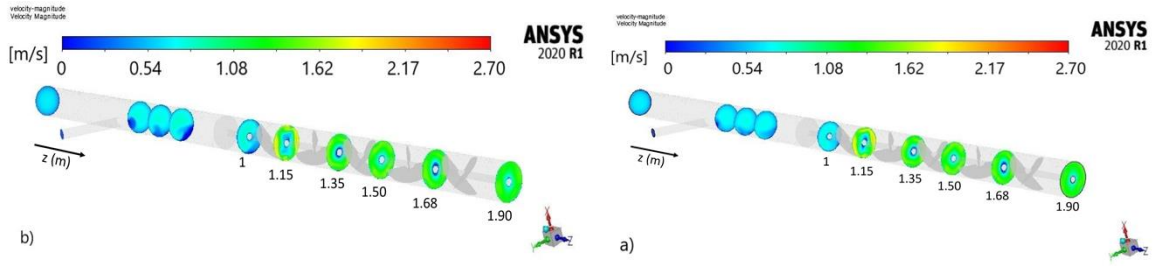

Figure 2: Velocity fields for 10 L/min *of additive flow rate: for a) E-W mixture, and b) E-G mixture*

The distribution of additive fluid was qualitatively analysed, for the three different binary mixtures and the three levels of additive flow rate considered, in the correspondence of a set of cross-sections. As a matter of fact, Figure 3 shows the concentration fields at *z* located between each mixing element of the static mixer. The average mass concentration of each mixture and the distribution of two components, for the same cross-section, are different. The differences in average mass concentration are more evident for the two cases of 10 and 20 L/min. On the outlet cross-section, where perfect mixing is guaranteed, it is possible to notice a slight colour gradient, which does not appear in the case of 1 L/min. For the same additive flow rate, the average mass composition, in each section, is influenced by the corresponding density of the additive fluid; since glycerol is denser than water, its average mass fraction is higher. The difference in density and viscosity also affects the distribution of additive along each cross-section. Overall, the concentration field for all scenarios shows a high degree of homogeneity, starting from the cross-section at *z* = 1.35 m, following the second mixing element. On the contrary, for *z* = 1 m and 1.5 m, the profile varies according to the mixture. As the flow rate of additive fluid increases, a progressive increase of the colour gradient is observed.

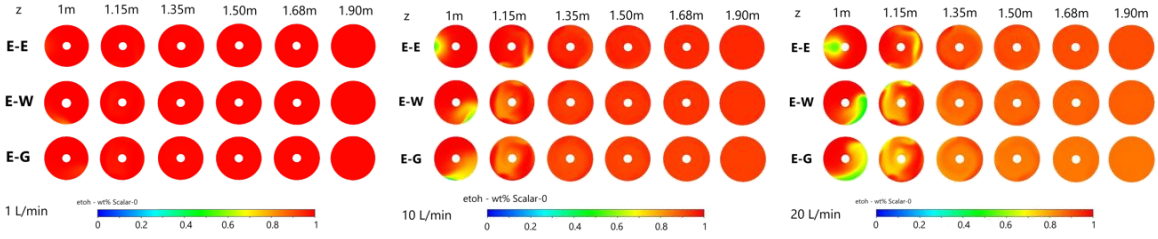

Figure 3: Concentration fields of the three binary mixtures for three levels of additive fluid.

From a quantitative point of view, the degree of mixing is computed with suitable Custom Field Functions (CFFs) to evaluate the standard deviation of the local mass fraction σ_b. The numerator of Eq(4) can be calculated as:

$$(\phi_i - \underline{\phi_b})^2 \rho_i u_i = (\phi_i - \underline{\phi_b})^2 \rho_{i,mix} u_z \tag{8}$$

where, ϕ_i is the local mass fraction related to the *i*-th cell, $\underline{\phi_b}$ is the average bulk mass fraction, determined from the mass balance and is a constant value, $\rho_{i,mix}$ is the local density of the mixture, which varies in function of the mass fraction and, finally, u_z is the local velocity in the flow direction.
A second CFF evaluates the denominator:

$$\rho_i u_i = \rho_{i,mix} u_z \tag{9}$$

which represents the product between density and local velocity.
For both functions, the integral averaged over area (AWA) at different cross-section is computed to determine the variance $\sigma_b^2(z)$ and then the degree of mixing $\delta_{mix}(z)$. Figure 4 compares the obtained profiles in the mixing of the two binary mixtures (E-W, E-G) and the reference E-E, for three levels of additive fluid flow rate.
To evaluate the contribution of the in-line static mixing elements on the mixing efficiency, a comparison with the corresponding empty-pipe scenarios was made. For the sake of simplicity, this analysis was carried out only for the E-W mixture. Figure 5 shows the comparison, for the three levels of additive fluid flow rate.

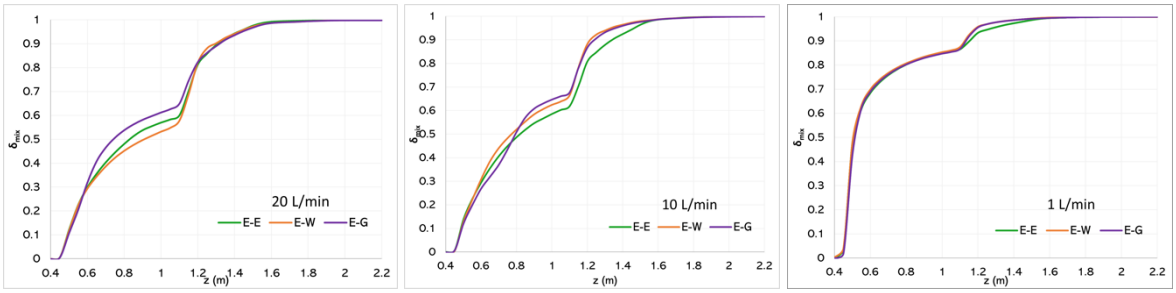

Figure 4: Profiles of degree of mixing for three binary mixtures and three levels of additive flow rate

It is evident how the presence of static mixers enhances efficiency; this effect is particularly evident at z = 1.1 m; before the first mixing element, values of δ_{mix} are almost superimposed. The obtained results confirm that without static mixers, the so-called perfect mixing (δ_{mix} > 0.95) cannot be guaranteed with the given pipe length.

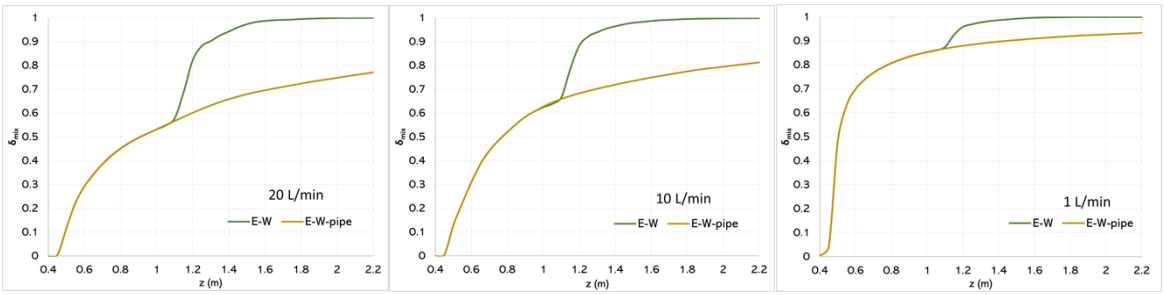

Figure 5: Profiles of degree of mixing for E-W mixture: comparison with the empty-pipe scenarios

From the CFD data, it was also possible to evaluate to what extent the type of mixture can influence the pressure drops. As a matter of fact, the static mixer elements introduce concentrated pressure drops which translate into an oscillatory trend of the absolute pressure profile. Figure 6 shows the comparison between the pressure profiles in the mixing of the three binary mixtures, for three levels of additive fluid flow rate. In all scenarios, with more evidence for the case of 20L/min, the greater deviation is observed for E-G mixture, compared to the E-W mixture. This effect can be assigned to the higher viscosity of the E-G mixture.

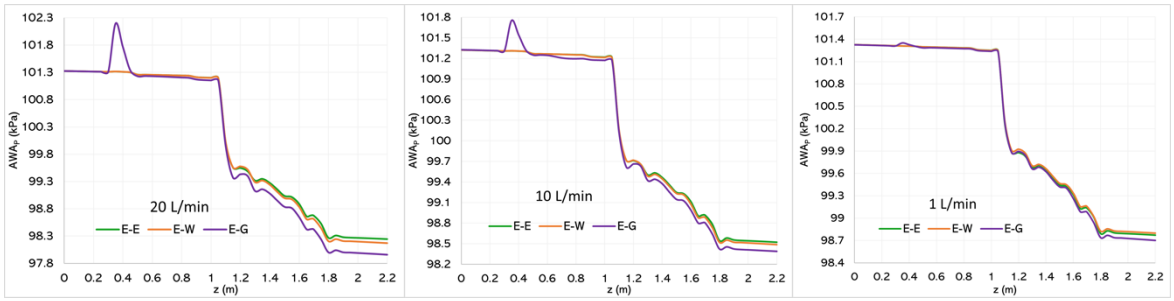

Figure 6: Profiles of pressure for three binary mixtures and three levels of additive flow rate

The results confirm that the introduction of static mixers increases the pressure drop; in addition, the pressure drops are strongly influenced by the density and viscosity of the mixture which depend on the composition itself. As an example, in the case of E-W mixture, the increase of pressure drops with respect to the empty-pipe scenario is equal to 18, 15, 15 times for the three values of additive flow rate (1, 10, 20 L/min), respectively.
Results from the numerical CFD simulations were then validated with the values obtained from the empirical correlations given by the manufacturing company (Ross, 2023). In particular, the following expression for each static mixer element was considered: $\Delta P_{el} = (0{,}008 Q^2 r \mu^{0{,}055})/D^4$, where Q is the total volumetric flow rate, r is the relative density of the mixture with respect to the reference liquid (water). The comparison results are resumed in Table 1. The deviation is significant; however, it is not surprising since the values used in the

correlation are equal to the average ones at the outlet section and since the analysed mixtures have highly non-ideal behaviour. Moreover, the thin-wall hypothesis, at the basis of the geometry modelling, can lead to a reduction of ΔP prediction. Nevertheless, the two sets of values have the same order of magnitude and CFD results can be considered acceptable. Therefore, further investigation is required, and a suitable experimental validation is to be organized.

Table 1: Comparison of pressure drops: CFD vs. empirical values

Case study	200-1 L/min		200-10 L/min		200-20 L/min	
Mixture	E-W	E-G	E-W	E-G	E-W	E-G
ΔP CFD [kPa]	2.42	2.50	2.69	2.80	3.00	3.15
ΔP emp [kPa]	6.41	6.41	7.20	7.22	8.10	8.30

5. Conclusions

In the present study, CFD analysis was employed to evaluate the performance of Ross LPD type static mixers, installed within an in-line mixer. The investigation was performed on two real binary mixtures obtained by combining the three main components of the sanitizing gel, i.e., ethanol-water and ethanol-glycerol. Each fluid was assumed with its real physical properties, e.g., the variation of density and viscosity, which depends on the mixture composition, was considered. To define a reference scenario, an ethanol-ethanol mixture was also analysed. As a result, the study has allowed the identification of the optimal operating conditions (degree of mixing and pressure drops). The condition of perfect mixing (δ_{mix} > 0.95) can be reached just after the second mixing element; this ensures that the real number (10) of mixing elements guarantees the mixture homogeneity between two consecutive fluid additions. Nevertheless, CFD simulations, despite being based on detailed models, cannot fully consider real process disturbances; therefore, a campaign of experimental validation is required. As future developments, input parameters for the setup of a digital twin of the real plant will be derived.

Acknowledgments

This research was funded by the POR FESR project 2014–2020 ‘TURBOFLUX’ promoted by the Tuscany region.

References

Alkindi A.S., Al-Wahaibi Y.M., Muggeridge A.H., 2008, Physical properties (density, excess molar volume, viscosity, surface tension and refractive index) of ethanol and glycerol, J. Chem. Eng. Data, 53, 2793–2796.

Sengupta D., Yelvington P., 2020, Advanced manufacturing progress: modular, intensified processes promote resilient manufacturing, www.aiche.org/resources/publications/cep/2020/june/advanced-manufacturing-progress-modular-intensified-processes-promote-resilient-manufacturing, accessed 12.02.2023.

Antognoli M., Galletti C., Bacci di Capaci R., Pannocchia G., Scali C., 2019, Numerical investigation of the mixing of highly viscous liquids with Cowles impellers, Chemical Engineering Transactions, 74, 973–978.

Forte G., Albano A., Simmons M., Stitt E.H., Brunazzi E., Alberini F., 2019, Assessing blending of non-newtonian fluids in static mixers by planar laser-induced fluorescence and electrical resistance tomography. Chem. Eng. Technol. 42, 1602-1610.

Ghanem A., Lemenand T., Della Valle D., Peerhossaini H., 2014, Static mixers: Mechanisms, application, and characterization methods, Chemical Engineering Research and Design, 57(11), 205–228.

Kuntz M., Menter F.R., Langtry R., 2003, Ten years of Experience with the SST turbulence model. In K. Hanjalic, Y. Nagano, and M. Tummers (Ed.), Turbulence, Heat and Mass Transfer, 4, 625–632.

Montante G., Coroneo M., Paglianti A., 2016, Blending of miscible liquids with different densities and viscosities in static mixers, Chemical Engineering Science, 141, 250–260.

Myers K.J., Bakker A., Ryan D., 1997, Avoid agitation by selecting static mixers, Chemical Engineering Progress, 93(6), 28–38.

Orsi G., Roudgar M., Brunazzi E., Galletti C., Mauri R., 2013, Water-ethanol mixing in T-shaped microdevices, Chemical Engineering Science, 95, 174–183.

Paul E.L., Atiemo-Obeng V.A., Kresta S.M. (Ed), 2004, Handbook of Industrial Mixing, Science and practice. 2004, John Wiley & Sons, Inc.

Ross. How to select a static mixer. www.staticmixers.com/motionless-howtoselect.asp, 12.02.2023.

Thakur R.K., Vial C., Nigam K.D.P., Nauman E.B., Djelveh G., 2003, Static mixers in the process industries - A review, Chemical Engineering Research and Design, 81(7), 787–826.